Kinetic theory of ion collection by probing objects in flowing strongly magnetized plasmas

K-S. Chung and I. H. Hutchinson
Plasma Fusion Center, Massachusetts Institute of Technology, Cambridge, Massachusetts 02139
(Received 2 March 1988)

A new one-dimensional collisionless kinetic model is developed for the flow of ions to probing structures in drifting plasmas. The cross-field flow into the presheath is modeled by accounting consistently for particle exchange between the collection flux tube and the outer plasma. Numerical solutions of the self-consistent plasma-sheath equations are obtained with arbitrary external ion temperature and parallel plasma flow velocity. Results are presented of the spatial dependence of the ion distribution function as well as its moments (density, particle flux, temperature, and power flux). The ion current to the probe is obtained and the ratio of the upstream to downstream currents is found to be well represented by the form $R = \exp(Ku_d)$, where $K \sim 1.7$ and u_d is the drift velocity in units of $\sqrt{(T_e/m_i)}$. The results are in good agreement with comparable recent fluid calculations but show substantial deviations from other models which ignore particle exchange out of the presheath. No evidence is found of the formation of shocks in the downstream wake, contrary to the implications of some fluid theories.

I. INTRODUCTION

The electrostatic probe is one of the fundamental techniques for measuring the properties of plasmas. In recent years it has found increasing use in fusion research as well as in more traditional applications, since it has been realized that the edge conditions are of great importance for magnetically confined plasmas. For example, the generation of impurities from the interaction of plasma with material edge structures is a vital issue for the achievement of clean and stable plasmas.[1] Also, edge conditions can influence the central energy confinement directly.[2]

One of the most important current applications is the diagnosis of plasmas which are flowing. Significant ion drift velocities can arise in the plasma-edge region of tokamaks and other magnetic confinement devices, for example, because of scrape-off flow toward a diverter plate or limiter surfaces.[3] Such plasma drifts may play an important role in confinement-related phenomena such as impurity transport, fluctuation levels, etc., and in the theory of divertors and limiters in fusion plasmas.[4]

Many measurements have shown large asymmetries in the ion saturation current drawn to probe faces parallel and antiparallel to the magnetic field.[5,6] These appear to be caused primarily by the presence of plasma flow along the field. When using diagnostic edge probes, such flows introduce a complicating factor which must be accounted for in probe data interpretation. More importantly, the asymmetry can be used to measure the flow velocity provided that a trustworthy theory of probe operation is available. It is the purpose of this work to contribute to the establishment of such a theory.

In fact, the physics of plasma flow to the probes used to measure edge plasma flows is largely the same as that involved in the flows themselves. Thus the present theory has relevance to the scrape-off physics itself as well as to probe interpretation.

Another application to which this theory relates is the interaction of rapidly moving bodies with plasmas. This is, of course, a longstanding problem. Planetary objects in the interplanetary plasma fall into this generic class. More recently, increased attention has focussed on man-made satellites, particularly in low-earth to ionospheric orbits. If the objects are large then magnetic field effects can be important and in some cases the present theory could be directly applicable. But some of the general features of our present approach are significant even for the situation in which the magnetic field can be ignored. Thus our theory may be applicable in part to many problems of the plasma "wake".[7–9] The upstream "ram"[10] tends to be less affected by the self-consistent electric fields and hence a less difficult problem, from the plasma viewpoint.

The theory of probe operation in magnetic fields is notoriously difficult. Bohm[11] obtained a criterion for stable sheath formation, assuming that ions are monoenergetic, and inferred a weak dependence of ion current upon ion temperature for $T_i < T_e$. This analysis has become a standard part of Langmuir probe theory.[12] However, his accompanying analysis of particle collection in magnetized plasmas took the processes to be diffusive in all dimensions and hence excluded most situations of interest where collisions are unimportant for parallel flow. Sanmartin[13] performed an asymptotic analysis of particle collection by spherical probes in a magnetic field for $T_i/T_e \sim 1$. He concentrated on the electron collection and treated ion collection as unperturbed by the magnetic field. Thus his theory, demonstrating the blurred knee in the current-voltage characteristic, is really only specifically relevant to cases where the ions are not strongly magnetized. Laframboise and Rubinstein[14] developed a theory of a cylindrical probe with an arbitrary angle to a uniform magnetic field for a completely collisionless plasma for arbitrary ion temperatures. The

difficulty here is that cross-field effects in most situations require some form of collisions for their proper modeling.

Our theory is addressed primarily to the case where the magnetic field is strong enough that the ion gyroradius is substantially smaller than the probing object. Specifically, we require that the ratio ρ_i/a be much less than 1, where $\rho_i=\sqrt{m_i T_i}/ZeB$ (with standard nomenclature) and a is the transverse probe dimension (typically the radius). For example, if $T_i=10$ eV, $B=4$ T, and $a=1$ mm, as might be typical of tokamak edge measurements, then for protons $\rho_i/a=0.08$ and the strong magnetic field condition is satisfied. In this case ion collection across the field is diffusive even if the parallel flow is dominated by inertial effects.[12] Thus the essential effect of the strong magnetic field is to introduce strong anisotropy in the ion dynamics.

As a result of the anisotropy, the quasineutral presheath region, where the acceleration of the ions occurs into the sheath, becomes highly elongated along the field, until the cross-field diffusion is able to balance the parallel collection flow. Figure 1 shows schematically the physical situation under consideration. The parallel collection flow velocity to the probe far exceeds the perpendicular diffusive flow. Therefore the detailed shape of the probe is unimportant; only the area of its parallel projection matters. Moreover, the perpendicular components of the momentum balance equation enter only into determination of the diffusive exchange rate of particles across the field. We shall find that this rate is important only in determining the presheath length. In view of these facts, a major simplification is possible: to regard the presheath as effectively one-dimensional. One can then seek solutions satisfying Poisson's equation and the Boltzmann equation in the parallel direction, treating the perpendicular diffusion equation as a source term in the parallel equations.

Theoretical treatments of the one-dimensional plasma sheath have a long history. Tonks and Langmuir[15] derived an integral equation for the potential variation in a collisionless plasma with a Boltzmann distribution of electrons. Harrison and Thompson[16] found an analytic solution for the plasma region and demonstrated that the sheath edge potential and current density are independent of the spatial variation of the source term when ions are born with zero energy.

Emmert *et al.*[17] extended their analysis to the case of finite ion temperature. They chose an energy-dependent source distribution function which would give rise to a Maxwellian ion distribution function if there were no electric field in the plasma. Bissel and Johnson[18] have solved same problem with different ion source distribution, corresponding to ionization of a Maxwellian distribution of neutral species. These two treatments give rise to noticeably different results, thus indicating the importance of the assumed source distribution. Besides, neither treatment gives results for the important situation of a plasma with parallel flow, where distributions with an appropriate flow velocity should be used.

Stangeby[19] has applied the kinetic calculation results of Emmert *et al.* directly to the theory of magnetized probes by assuming that cross-field transport can be modeled as a source in the one-dimensional parallel equations. He has also given[20] a one-dimensional fluid calculation which proves to be analytically integrable even with plasma flow incorporated in the source. In either case the ion source adopted corresponds to "birth" of ions within the collection region considering only the cross-field transport of ions "into" the flux tube.

Recently Hutchinson[21] has investigated a fluid approach that uses a more physically appropriate source, accounting not only for ions moving "into" the collection region, but also for ions moving "out." In the context of a one-dimensional model this implies a sink of ions characteristic of the inner presheath as well as a source of ions characteristic of the external plasma. As Hutchinson shows, this modification corresponds to adopting a realistic value of ion viscosity rather than making it effectively zero, as Stangeby's approach does. In a further study,[22] Hutchinson has explored the effects of adopting different values of the viscosity and shown that the results of Stangeby are in reality a singular case, not relevant to any finite viscosity. In addition, this latter work includes a two-dimensional calculation which shows excellent agreement with the one-dimensional approximation.

These latest fluid analyses offer a substantially more accurate and reliable basis for understanding the interaction of probes with flowing magnetized plasmas. However, they cover only the subsonic regime and approximate the ion energy equation in a way that is rigorously accurate only if the ions are isothermal, which they usually are not. Naturally, also, they provide no information on the ion distribution function or related important quantities such as heat flux within the presheath.

It is the purpose of this work to analyze the problem by using a one-dimensional collisionless kinetic analysis but accounting correctly for the diffusive nature of the ion source. In this way we obtain ion distribution infor-

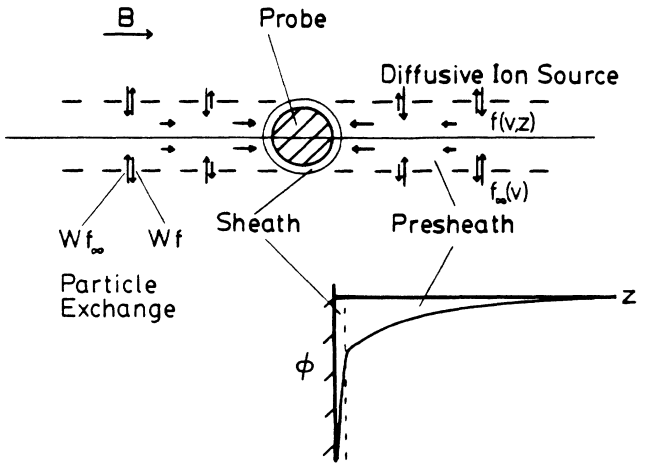

FIG. 1. Schematic illustration of the geometry of the ion collection region. Ions accelerate toward the probe inside the presheath while the exchange of ions between the presheath and the outer plasma acts as a (diffusive) source in the one-dimensional equations of motion.

mation and provide an alternative formulation to compare with the fluid calculations. We find in general very satisfactory agreement with Hutchinson's[23] fluid calculations at the subsonic plasma flow speeds for which they are available. In addition, the present model gives clear results well into the supersonic flow regime.

In Sec. II we set up the kinetic model which contains "transport" source terms. Section III deals with the numerical method used to solve the plasma-sheath equation. In Sec. IV we present and discuss our results which, in addition to the ion distribution function, include ion current, temperature, fluid velocity, density, power flux, and ratio of upstream to downstream current. Potential variations are also included. Section V gives our conclusions.

II. MODEL

A. Governing equations

The one-dimensional governing equations of ions in the presheath (including the sheath) can be described by the Boltzmann equation, which is given by

$$\left[\frac{\partial}{\partial t}+v_z\frac{\partial}{\partial z}+a_z\frac{\partial}{\partial v_z}\right]f(z,v_z,t)=C_f+S_f\ , \tag{1}$$

where $f(z,v_z,t)$ is the one-dimensional ion distribution function, z is position along the magnetic field, v_z is the parallel velocity of ions, a_z is the acceleration of the ions governed by the Lorentz force, C_f is the collision operator, and S_f is the volume source of ions. Assuming steady state ($\partial/\partial t=0$), and ignoring collisions ($C_f=0$), the Boltzmann equation can be written as

$$\left[v_z\frac{\partial}{\partial z}-\frac{q}{m}\frac{d\phi}{dz}\frac{\partial}{\partial v_z}\right]f(z,v_z)=S_f\ . \tag{2}$$

Here m, q, and ϕ are ion mass, ion charge, and electric potential, while S_f will be taken as the ion source due to cross-field transport. The energy equation, governing the phase space orbits, is

$$\tfrac{1}{2}mv_z^2+q\phi(z)=E\ , \tag{3}$$

where E is the constant total energy.

The electrons are assumed to be isothermal, described by the Boltzmann relation

$$n_e(z)=n_\infty e^{e\phi(z)/T_e}\ , \tag{4}$$

where n_∞ and T_e are electron density and temperature, and subscript infinity refers to values outside the presheath.

The electron and ion densities are related by Poisson's equation, i.e.,

$$\frac{d^2\phi}{dz^2}=-\frac{1}{4\pi}\left[q\int f(z,v)dv-en_e(z)\right]\ . \tag{5}$$

The expected variation in the plasma potential and corresponding orbit is shown schematically in Fig. 2.

The cross-field transport is considered to be governed by a frequency $W(z,v)$, which gives the rate at which particles are exchanged between the presheath and the outer plasma, so the source due to cross-field transport becomes

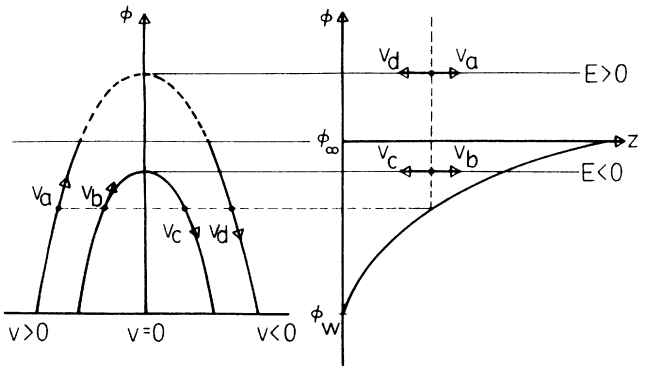

FIG. 2. Illustration of the particle orbits and plasma potential variation. The potential can be considered as the independent variable when plotting the particle orbits, which are then parabolic. The task of the solution procedure is to find the spatial variation of the potential that self-consistently satisfies the equations.

$$S_f=W(z,v)[f_\infty(v)-f(z,v)]\ . \tag{6}$$

The first term on the right-hand side represents the ions entering the collection flux tube from the outside. The second term is the new term that we are introducing. It represents ions being exchanged out of the collection flux tube, as indicated schematically in Fig. 1. The exchange rates (the W's) for these two processes are taken to be equal, representing random migration of ions in either direction. The rate is related via

$$W\simeq\frac{D}{a^2} \tag{7}$$

to D, the anomalous cross-field diffusion coefficient.

B. Nondimensionalization

If we assume that $W(z,v)$ is independent of v, the equations can be nondimensionalized by using the following transformations. We define a type of ion acoustic speed, ignoring the ion pressure, by

$$V_s\equiv\left[\frac{ZT_e}{m}\right]^{1/2}\ , \tag{8}$$

where $Z=q/e$, and then define a characteristic length as

$$L_\parallel\equiv\frac{V_s}{W(z)}\ . \tag{9}$$

This is the characteristic length of the presheath, but in general varies with parallel position if W does. Then the nondimensional forms of the parameters are

$$\begin{aligned} &x\equiv\int\frac{W(z)}{V_s}dz,\quad u\equiv\frac{v}{V_s}\ ,\\ &\eta\equiv-\frac{e\phi}{T_e},\quad \varepsilon\equiv\frac{E}{ZT_e}\ ,\\ &\lambda(x)\equiv\frac{\lambda_D}{L_\parallel(x)},\quad g(x,u)\equiv\frac{V_s}{n_\infty}f(z,v)\ , \end{aligned} \tag{10}$$

where λ_D is the Debye length. In terms of these parameters the equations become

$$\left[u\frac{\partial}{\partial x}+\frac{d\eta}{dx}\frac{\partial}{\partial u}\right]g(x,u)=g_\infty(u)-g(x,u)\ , \tag{11}$$

$$\varepsilon=\frac{u^2}{2}-\eta\ , \tag{12}$$

$$\lambda^2(x)\frac{d^2\eta}{dx^2}=Z\int g(x,u)du-e^{-\eta(x)}\ . \tag{13}$$

If the external ion distribution is Maxwellian with temperature T_i, shifted by a velocity v_d, then

$$g_\infty(u)=\left[\frac{ZT_e}{2\pi T_i}\right]^{1/2}\exp[-ZT_e(u-u_d)^2/2T_i]\ . \tag{14}$$

The boundary conditions on the distribution function are

$$g(x=0,\ u\geq 0)=0,\quad g(x=\infty,\ u)=g_\infty(u)\ , \tag{15}$$

which means that the probe has a perfectly absorbing surface and the ion distribution has Maxwellian form outside the presheath. Those on the potential are

$$\eta(x=0)=\eta_w,\quad \eta(x=\infty)=0\ . \tag{16}$$

The operator of the Boltzmann equation (11) can be written as

$$u\frac{\partial}{\partial x}+\frac{d\eta}{dx}\frac{\partial}{\partial u}=\frac{d\eta}{dx}\left[u\frac{\partial}{\partial\eta}+\frac{\partial}{\partial u}\right]$$
$$=\frac{d\eta}{dx}\left[\frac{d\eta}{du}\frac{\partial}{\partial\eta}+\frac{\partial}{\partial u}\right]=\frac{d\eta}{dx}\frac{D}{Du}\ ,$$

where D/Du is the convective derivative along the orbit of constant total ion energy. Then the kinetic equation is

$$\frac{Dg}{Du}=\frac{1}{d\eta/dx}[g_\infty(u)-g(x,u)]\ . \tag{17}$$

Since the ratio (λ) of the Debye length to ion collection length is typically $\ll 1$, very fine resolution is needed near the sheath region. To provide this without increasing the number of mesh points excessively, we choose a nonuniform meshing along the x direction like that of Emmert *et al.*[17] Putting

$$x=s^\delta\quad(\delta>1)\ , \tag{18}$$

Eqs (11) and (13) become

$$\frac{Dg}{Du}=\frac{\delta s^{\delta-1}}{d\eta/ds}[g_\infty(u)-g(s,u)]\ , \tag{19}$$

$$\left[\frac{\lambda}{\delta}\right]^2\left[\frac{1}{s^{2\delta-2}}\frac{d^2\eta}{ds^2}-\frac{\delta-1}{s^{2\delta-1}}\frac{d\eta}{ds}\right]=\rho(s)\ , \tag{20}$$

with

$$\rho(s)=Z\int g(s,u)du-e^{-\eta(s)}\ . \tag{21}$$

Then we use a mesh that is uniform in s.

By taking the moments of the ion distribution we can get the ion density, current, fluid velocity, temperature, and power flux as

$$n(x)=\int g(x,u)du\ , \tag{22}$$

$$J(x)=\int ug(x,u)du\ , \tag{23}$$

$$V(x)=J(x)/n(x)\ , \tag{24}$$

$$T(x)=\frac{1}{n(x)}\int[u-V(x)]^2g(x,u)du\ , \tag{25}$$

$$P(x)=\int(\tfrac{1}{2}u^2)ug(x,u)du\ . \tag{26}$$

These are, of course, in normalized nondimensional form.

III. NUMERICAL METHOD

To solve the preceding equations, we guess an initial potential variation (η_i). Along each energy orbit (ε_j), velocity sets are obtained as

$$u_{i,j}=\sqrt{2(\varepsilon_j+\eta_i)}\ , \tag{27}$$

where i is the position index ($1\leq i\leq N_p$) and j is the orbit (energy) index ($1\leq j\leq N_e$) with a total of N_p positions and N_e orbits.

We obtain the ion distribution function along the orbits by solving the kinetic equation with a semi-implicit method, i.e.,

$$g_{i+1,j}=\frac{p_ih_{i,j}g_{\infty i,j}+[1-(1-\psi)p_ih_{i,j}]g_{i,j}}{1+\psi p_ih_{i,j}}\ , \tag{28}$$

where

$$p_i=\frac{\delta s_i^{\delta-1}}{(d\eta/ds)|_i},\quad h_{i,j}=u_{i+1,j}-u_{i,j}\ ,$$

and ψ is a mixing parameter. (If it is equal to 1, 0.5, and 0, the scheme is implicit, semi-implicit, and explicit, respectively. We use $\psi=0.5$ throughout our calculations.) The boundary conditions are

$$g_{1,j}=0,\quad g_{N_p,j}=g_{\infty i,j}\ . \tag{29}$$

Because of the shape of the orbits and the fixed position grid, the velocity spacing between adjacent points on an orbit is large near $u=0$. In order to minimize the numerical error which otherwise arises in the orbit integration, we introduce an additional point on the orbit at $u=0$. The value of potential there is appropriately interpolated between the adjacent points on the position mesh. This greatly improves the accuracy of the distribution function on the negative-velocity side. We obtain the ion density by integrating the ion distribution over velocity space at each position.

Since the Poisson equation [Eq. (20)] is an elliptic equation, we are able to solve it by the successive over-relaxation method[24] for nonuniform meshing in x (but uniform mesh in s). The scheme for the potential is

$$\eta_i^{\mu+1}=[-\omega_iA_i\eta_{i-1}^{\mu+1}+(1-\omega_i)B_i\eta_i^\mu-\omega_iC_i\eta_{i+1}^\mu$$
$$+\omega_i\rho_i]/B_i\ , \tag{30}$$

where

$$B_i = -2\left[\frac{\lambda}{\delta\,\Delta s}\right]^2$$

and

$$A_i = C_i = -\tfrac{1}{2}B_i[1+(\delta-1)s_i\Delta s/2]\ .$$

Here ρ_i is charge density at position i, ω_i is a generalized relaxation parameter which we take equal to 1.9λ, $\Delta s = L/(N_p-1)$, where L is the total length of the flux tube, and μ is an iteration index.

For the quasineutral case ($\lambda=0$), Eq. (20) can be used to obtain the potential directly as

$$\eta_i^{\mu+1} = -Z\ln[n_i(\eta_i^{\mu})]\ . \tag{31}$$

However, direct iteration schemes of this type are usually unstable.[25] Instead, a relaxation scheme has been used,

$$\eta_i^{\mu+1} = \eta_i^{\mu} + \omega\ln(n_e/n_i)\ , \tag{32}$$

where ω is a relaxation parameter, which we take to be 0.1.

We obtain self-consistent solutions for the potential and the ion distribution function by iterating these procedures until they reach a convergence criterion

$$\max|\,\eta_i^{\mu+1}-\eta_i^{\mu}\,| < \epsilon\ ,$$

where ϵ is a small positive number. After getting the self-consistent ion distribution and potential variation, the moments of the ion distribution (density, flux, fluid velocity, temperature, and power flux) are obtained by Simpson-rule integration of the ion distribution over the nonuniform velocity space.

IV. RESULTS AND DISCUSSION

For the following results we use singly charged ions, $Z=1$, nonuniformity of distance, $\delta=2.5$, convergence criterion $\epsilon\sim10^{-4}$, position mesh $N_p=51$, and energy mesh $N_e=100$. The negative sign in ion fluid velocity, current, and power flux denotes motion toward the probe surface.

A. Drift-free plasma results

We give first some results when there is no ion drift ($u_d=0$) for a case with $T_{i\infty}=T_e$. In Fig. 3 are shown the variation versus nondimensional distance of the potential, ion density, ion temperature, fluid velocity, power flux, and ion current. Figure 4 shows the ion distribution at different potentials and hence positions. These results are essentially the direct analog of those of Emmert *et al.*[17] and Bissel and Johnson.[18] Because of our different treatment, however, we find that the potential perturbation is noticeably larger in our case and consequently the density falls off toward the probe more rapidly. These differences are a consequence of the fact that our inclusion of exchange of particles out of the collection flux tube constitutes a loss of momentum. In order to accelerate the ions to enter the sheath at the sound speed then requires a greater potential drop than if the momentum loss is ignored.

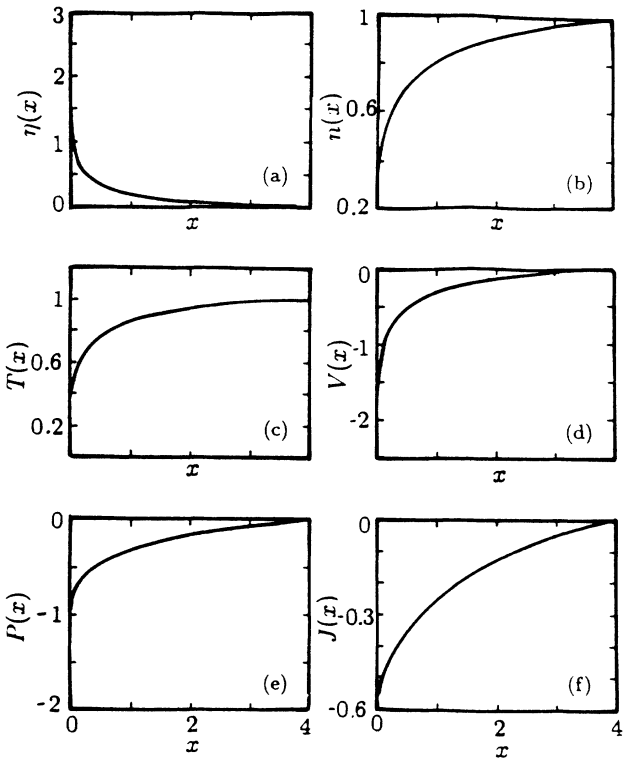

FIG. 3. Overall ion parameters. (a) Potential variation; (b) ion density; (c) temperature; (d) fluid velocity; (e) power flux; (f) current along the flux tube for $\lambda=0.001$, $u_d=0$, $T_{i\infty}=T_e$, $\eta_w=3$.

In Fig. 5 we show the variation of the results with different values of the ratio of Debye length to collection length (λ). These show, as expected, that cases with small λ, e.g., 0.001, are indistinguishable from the quasineutral case, except actually within the sheath. This agreement is a useful verification of the two different Poisson solver schemes used. The distribution functions shown here are those at the sheath edge. For the

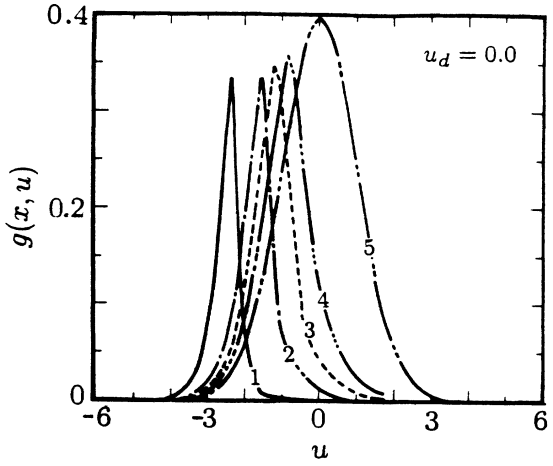

FIG. 4. Ion distribution functions at different potentials, $\eta=3$ (curve 1), 1.45, 0.87, 0.57, and 0 (curve 5) for $\lambda=0.001$, $u_d=0$, $T_{i\infty}=T_e$, $\eta_w=3$. Curve 3 is the distribution at the sheath.

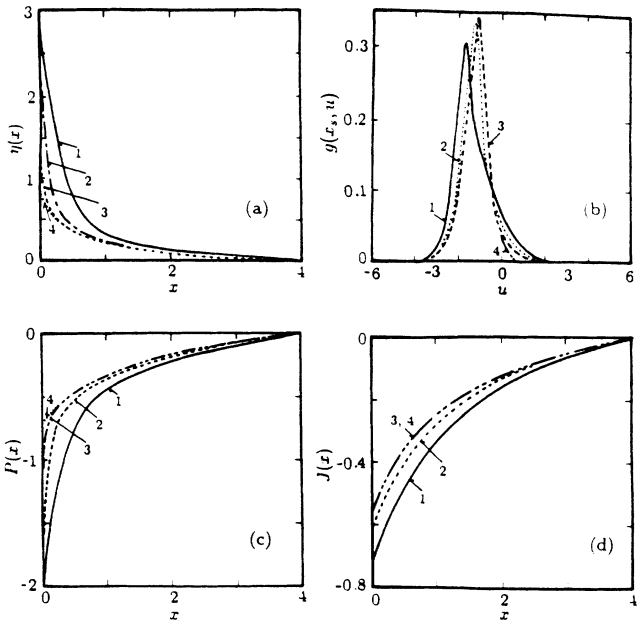

FIG. 5. (a) Potential variations, (b) sheath ion distributions, (c) power fluxes, (d) currents with different λ [$=0.1$ (curve 1), 0.01 (curve 2), 0.001 (curve 3), and 0 (curve 4)] for $u_d=0$, $T_{i\infty}=T_e$, $\eta_w=3$.

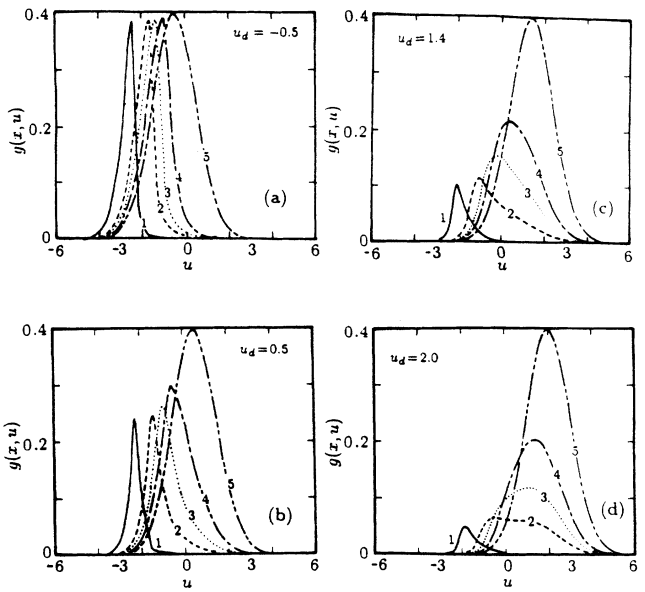

FIG. 6. Ion distribution functions for different ion drift velocities, (a) $u_d=0.5$, (b) $u_d=0.5$, (c) $u_d=1.4$, (d) $u_d=2.0$ when $\lambda=0.001$, $T_{i\infty}=T_e$, $\eta_w=3$. $\eta_1=\eta_w$, $\eta_2\simeq\frac{1}{2}\eta_w$, $\eta_3\simeq\frac{1}{3}\eta_w$, $\eta_4\simeq\frac{1}{4}\eta_w$, $\eta_5=\eta_\infty$ (subscripts 1–5 correspond to curves 1–5).

plasma-sheath equations ($\lambda>0$), the sheat edge is defined as the position where the ion fluid velocity [$V(x)$] is the same as the ion acoustic velocity (C_s) toward the probe surface, which is defined by

$$C_s=\sqrt{(T_e+T_{is})/m_i}\ , \tag{33}$$

where T_{is} is the ion temperature at the point where $V(x)=V_s(\equiv\sqrt{T_e/m_i})$. For the quasineutral case ($\lambda=0$) the sheath edge is at the mesh-point adjacent to the boundary. In our results hereafter we use either $\lambda=0.001$ or the quasineutral forms. These give essentially identical results that are independent of the value assumed for the wall potential, provided the wall is more negative than the sheath-edge potential ($\eta_w>\eta_s$).

B. Drift velocity effects: variation along the flux tube

We now give a series of results for $T_{i\infty}=T_e$ with different drift velocities of the external plasma. In Fig. 6 are shown the ion distributions at various points along the collection flux tube for four different drift velocities, $u_d=-0.5$, 0.5, 1.4, 2.0. We also give the potential variations (Fig. 7), ion currents (Fig. 8), ion temperatures along the presheath (Fig. 9), power flux, and fluid velocity (Fig. 10) for subsonic and transonic ion drift velocities ($-1.4\le u_d\le 2.5$). For cases with ions drifting toward the probe ($u_d<0$), the length of the collection region decreases. Parameters other than temperature vary smoothly even with transonic drift.

When $u_d<0$, the temperature variation along the flux tube is monotonically increasing. However, with strong drift away from the probe, it is mostly decreasing. Intermediate cases have some oscillations (e.g., $u_d=0.5$ in Fig. 9) along the flux tube. This kind of variation is common to both plasma-sheath ($\lambda>0$) and plasma-equation ($\lambda=0$) treatments, and with different ion temperatures outside the presheath ($T_{i\infty}=0.2,1,2T_e$). These oscillations are of uncertain physical significance and may in part arise from the discreteness of our distribution-function representation. Referring to Fig. 6, one can see that there is a balance between the acceleration due to the electric field, which draws the ions to the probe, and the influx of ions with the external velocity distribution. If the external flow is towards the probe, the distribution tends to narrow. If it is away from the probe, so that the external and internal flow velocities are opposite, the distribution tends to get wider. This change of the ion dis-

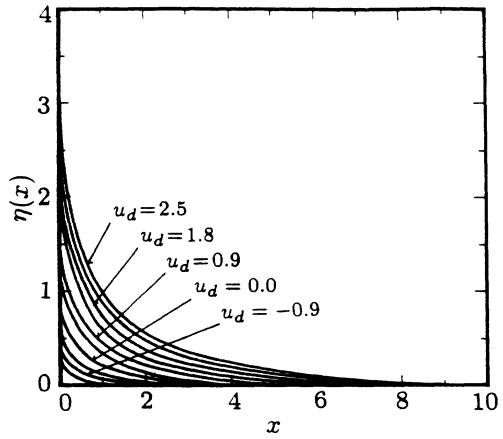

FIG. 7. Potential variations with different drift velocities, $u_d=-1.4$, -0.9, -0.5, 0.0, 0.5, 0.9, 1.4, 1.8, 2.2, and 2.5, for $\lambda=0$, $T_{i\infty}=T_e$, and $\eta_w=5$.

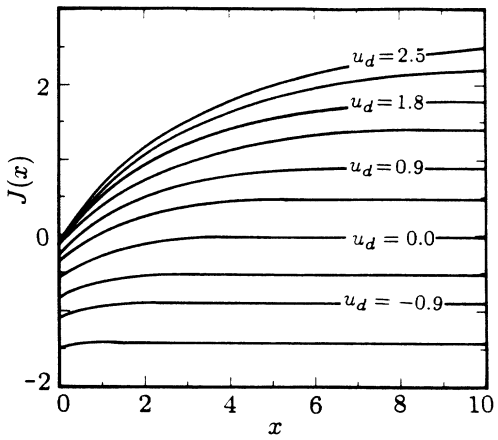

FIG. 8. Ion current variations with different drift velocities, $u_d=-1.4$, -0.9, -0.5, 0.0, 0.5, 0.9, 1.4, 1.8, 2.2, and 2.5, for $\lambda=0$, $T_{i\infty}=T_e$, and $\eta_w=5$.

tribution along the flux tube with different ion drift velocities (Fig. 9) is what the ion temperature variation along the flux tube is showing.

Fluid treatments generally show singularities, which are interpreted as indicative of shock formation, when the drift velocity exceeds the sound speed. In Figs. 7–10, however, there is no evidence of a shock for the transonic case and this remains true, as further code runs have shown, even up to $u_d=5$. Substitution of our solutions indicates that the theoretical necessary conditions for rarefaction shock[26–28] are not satisfied. Thus the absence of shocks seems to be consistent, although we know of no *a priori* argument why there should be none. It seems likely that it is the damping inherent in a proper kinetic treatment, which is absent from the fluid models, that prevents shock formation. If so, then results for transonic and supersonic velocities require a kinetic treatment such as ours.

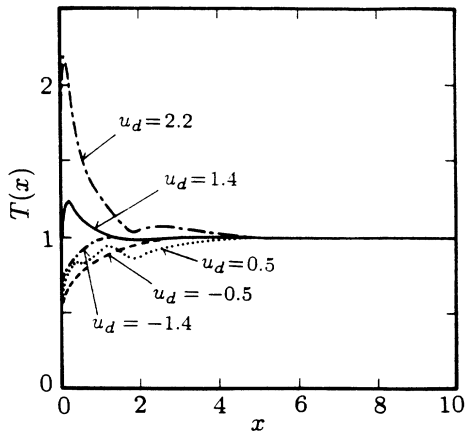

FIG. 9. Ion temperature with different drift velocities, $u_d=-1.4$, -0.5, 0.5, 1.4, and 2.2, for $\lambda=0$, $T_{i\infty}=T_e$, and $\eta_w=5$.

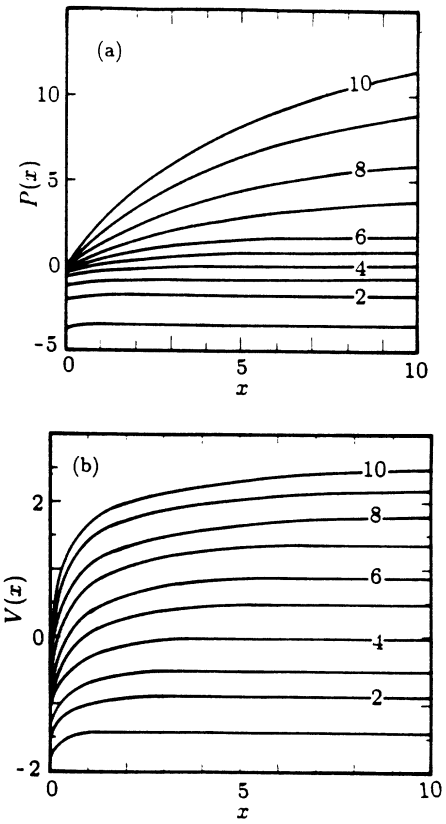

FIG. 10. (a) Power flux and (b) fluid velocity variation with different drift velocities $u_d=-1.4$ (curve 1), -0.9, -0.5, 0.0, 0.5, 0.9, 1.4, 1.8, 2.2, and 2.5 (curve 10), for $\lambda=0$, $T_{i\infty}=T_e$, and $\eta_w=5$.

C. Drift-velocity effects: sheath parameters

For the purposes of interpreting the interaction of the plasma with material objects it is the values of the parameters at the wall (material surface) that matter most. However, some of these values are dependent on the wall potential so it is difficult to give compact general results for the wall value. Adopting a wall potential that gives zero total electric current (the floating potential) is a special value that is often adopted but by no means generally appropriate. Our approach is to take advantage of the fact that for $\lambda \ll 1$ the sources within the sheath are negligible. Therefore the values of the ion parameters at the wall are related to those at the sheath edge via a trivial transformation: an energy- and flux-conserving fall through a potential drop equal to the difference between wall and sheath potential. This means, of course, that the wall ion flux is the same as the flux at the sheath edge. Other parameters for any wall potential (more negative than the sheath potential) can be calculated from the sheath values that we give.

Figure 11 shows ion distributions at sheath for $T_{i\infty}=T_e$ with different drift velocities. The similarities in shape for the different drift velocities are an indication of the fact that the ions tend to flow into the sheath at the sound speed, regardless of external flow. The different to-

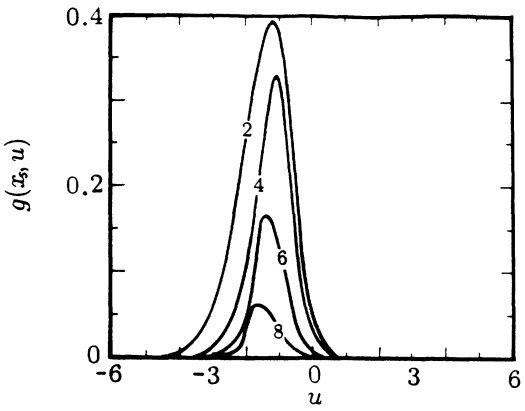

FIG. 11. Ion distributions at sheath with different drift velocities, $u_d=-0.9$ (curve 2), 0.0 (curve 4), 0.9 (curve 6), and 1.8 (curve 8) for $\lambda=0$, $T_{i\infty}=T_e$, and $\eta_w=5$.

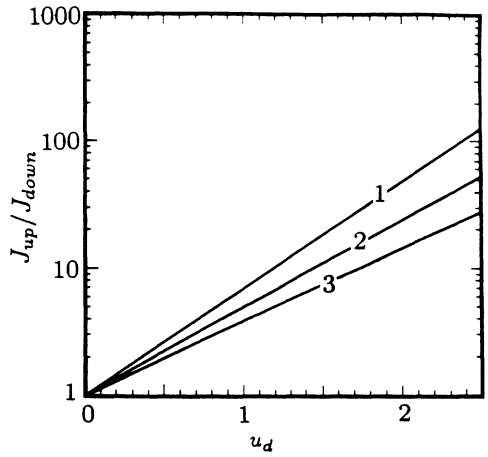

FIG. 13. Ratio of upstream to downstream current into the sheath, for $-1.4\le u_d\le 2.5$, $\lambda=0$, $T_{i\infty}=0.2T_e$ (curve 1), $1.0T_e$ (curve 2), $2.0T_e$ (curve 3), and $\eta_w=5$.

tal heights show the density reduction when the external drift is away from the probe. In Fig. 12 we show the ion current flowing into the sheath as a function of external drift velocity, for three values of ion temperature. The dependence on T_i is noticeable but not large.

The diagnosis of plasma flow via "Mach" probes[5] requires interpretation of the ratio of the ion collection currents to the upstream and downstream faces of the probe. Therefore in Fig. 13 we give this ratio; it increases as $|u_d|$ and $T_{i\infty}$ get larger. The values obtained follow curves which are remarkably straight on the log-linear plot of Fig. 13. Thus the ratio can be expressed as

$$R\equiv\frac{J_{\rm up}}{J_{\rm down}}=e^{Ku_d}\ , \tag{34}$$

where $K\sim 1.9$, 1.7, 1.3 for $T_{i\infty}=0.2T_e, 1.0T_e, 2.0T_e$, respectively. For ion drift beyond the range of Fig. 13, up to 5, the ratio values were found to rise slightly above the straight-line fits.

Figure 14 gives the other parameters of interest at the sheath edge. The sheath potential is important in defining the sheath potential drop for given wall potential (relative to the plasma). At zero drift velocity, it proves to be only weakly dependent on the external ion temperature, with a value quite close to the Harrison and Thompson[16] value, 0.854. For subsonic ion drift flows ($|u_d|<1$), the ion temperature at the sheath has smaller values than outside the presheath. This is an interesting result because most previous fluid treatments assume that there is no temperature gradient along the presheath. Our results show that this is a bad approximation. The temperature appears to satisfy approximately an adiabatic law: $pn^{-\gamma}=$const, with $\gamma=2$–2.5.

For transonic ion drift away from the probe, sheath ion

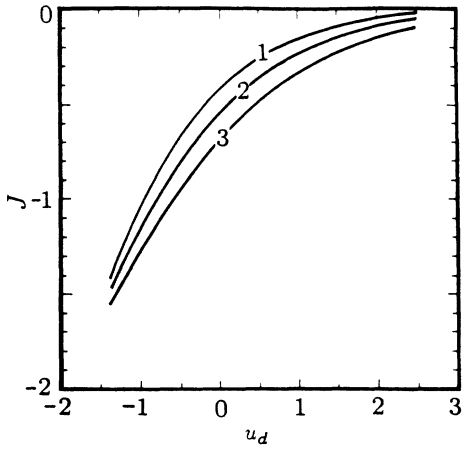

FIG. 12. Sheath current for $-1.4\le u_d\le 2.5$, $\lambda=0$, when $T_{i\infty}=0.2T_e$ (curve 1), $1.0T_e$ (curve 2), $2.0T_e$ (curve 3), and $\eta_w=5$.

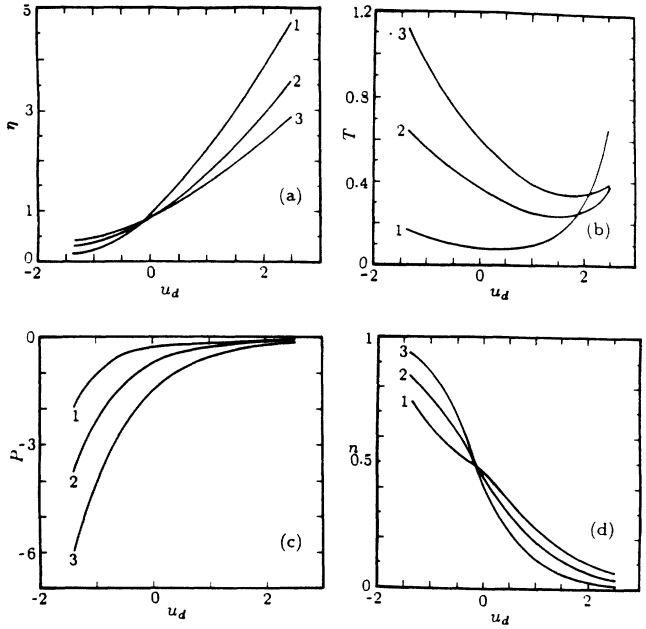

FIG. 14. Sheath (a) potential, (curve 3) (b) temperature, (c) power flux, and (d) density, for $-1.4\le u_d\le 2.5$, $\lambda=0$, $T_{i\infty}=0.2T_e$ (curve 1), $1.0T_e$ (curve 2), $2.0T_e$ (curve 3), and $\eta_w=5$.

temperature increases again, as we have previously discussed. This effect for large drift is stronger when $T_{i\infty}$ is small. When the ion temperature outside the flux tube is $0.2T_e$, the sheath temperature is larger than that of $1.0T_e$ and $2.0T_e$ for the largest drift velocities.

As an example of a transonic flow case, the variation with position along the flux tube of potential, density, temperature, fluid velocity, power flux, and current are given in Fig. 15 for $T_{i\infty}=0.2T_e$, $1.0T_e$, and $2.0T_e$, with $u_d=2.5$.

Figure 16 shows an expansion of the temperature variations near the sheath and their corresponding ion distributions. For low ion temperature and large ion drift (e.g., $T_{i\infty}=0.2T_e$ and $u_d=2.5$), there appears a double-humped ion distribution near the sheath. Clearly the significance of attaching a temperature to such pathological distributions is doubtful.

D. Comparison of sheath currents with other treatments

Figure 17 shows a comparison of the results of different kinetic analyses.[11,16–18] Since ours are really the first results to include ion drift we show only results for zero ion drift. With the exception of Bohm's finite-ion-energy calculation, which is for a spherical probe, the models are one-dimensional plane-geometry cases. As anticipated, our model gives somewhat lower currents than the other models, because we have included the ion momentum loss due to particle exchange. [Note: In the original papers of Emmert *et al.* and Bissel and Johnson, the current was normalized by

$$n_\infty\sqrt{2T_{i\infty}/\pi m_i}$$

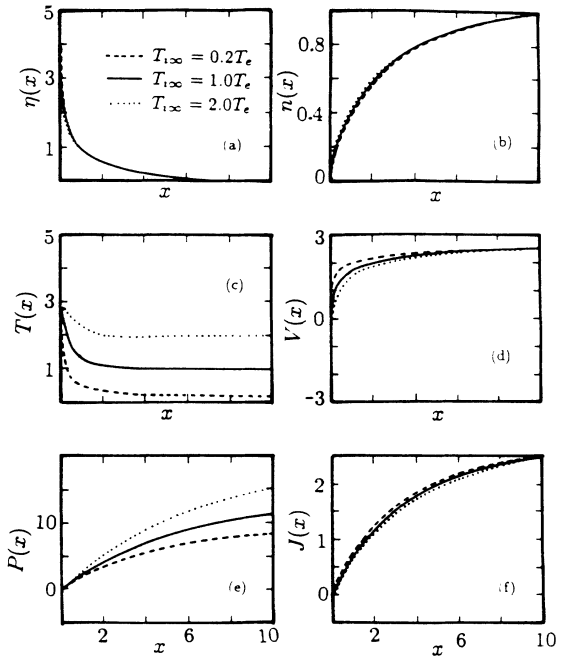

FIG. 15. (a) Potential, (b) density, (c) temperature, (d) velocity, (e) power flux, and (f) current as a function of position for $u_d=2.5$, $\lambda=0$, $T_{i\infty}=0.21T_e$, $1T_e$, $2T_e$, and $\eta_w=5$.

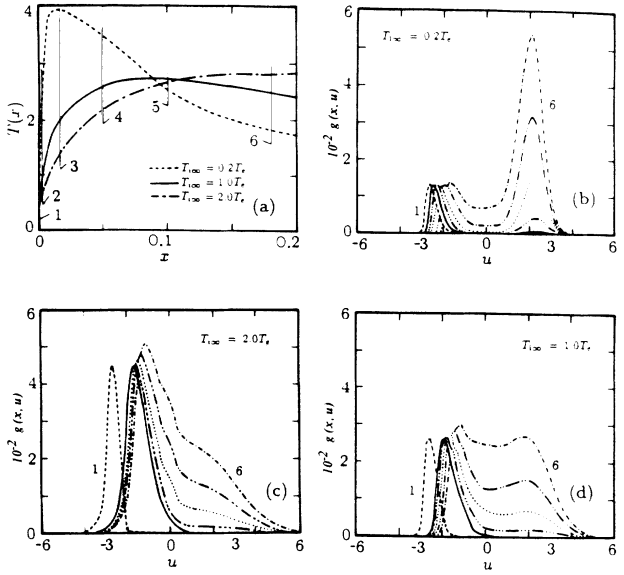

FIG. 16. (a) Temperature variation and (b)–(d) corresponding ion distributions near sheath for $u_d=2.5$, $\lambda=0$, $\eta_w=5$, and three external temperatures (b) $T_{i\infty}=0.2(b)$, (d) $T_{i\infty}=1T_e$, and (c) $T_{i\infty}=2T_e$. Positions 1 to 6 are as follows: $x_1=0$, $x_2=0.0032$, $x_3=0.018$, $x_4=0.05$, $x_5=0.1$, and $x_6=0.18$.

and

$$n_\infty\sqrt{(T_{i\infty}+T_e)/m_i}\ ,$$

respectively. In their normalization their results show a decrease of current with $T_{i\infty}$. However, the currents are increasing with $T_{i\infty}$ when they are normalized by our definition of ion sound speed ($V_s=\sqrt{T_e/m_i}$)].

In Fig. 18 we compare the sheath currents calculated here with those of fluid models,[20,21] which give results with finite ion drift. The fluid results are expressed in

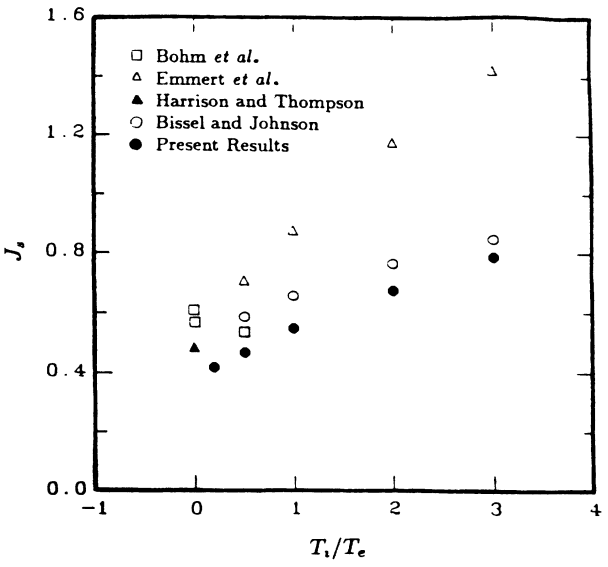

FIG. 17. Sheath-current variations with zero drift ($u_d=0$) for $0<T_{i\infty}/T_e<3$ from various theories.

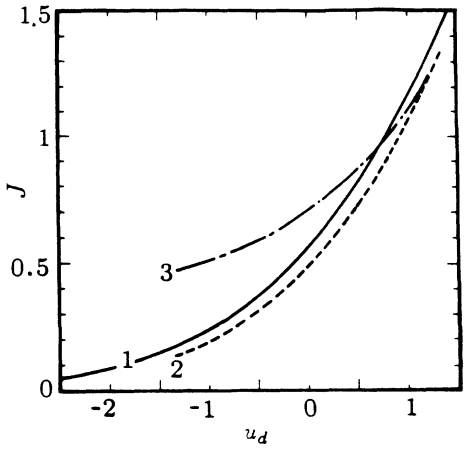

FIG. 18. Sheath-current variations with drift ($-1.4 \leq u_d \leq 2.5$), for $T_{i\infty} = T_e$. Curve 1, present results; curve 2, fluid model of Hutchinson; curve 3, fluid model of Stangeby.

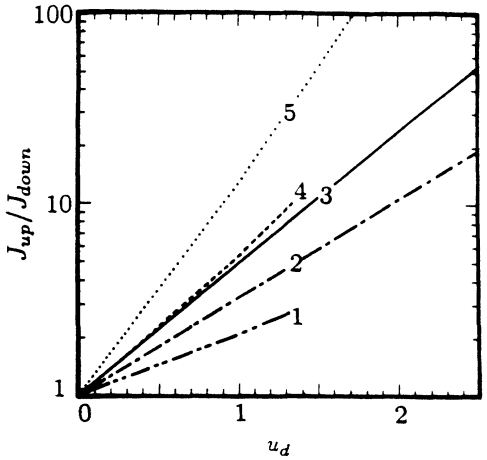

FIG. 19. Comparison of the upstream to downstream ratio of sheath currents from various models, for $T_{i\infty} = T_e$. Curve 1, Stangeby; curve 2, Proudfoot *et al.*; curve 3, present results; curve 4, Hutchinson; curve 5, Mott-Smith and Langmuir.

units normalized by the "ion acoustic velocity." This is not the same as our parameter V_s, which includes only T_e not T_i [see Eq. (8)]. Thus there is a degree of ambiguity in the comparison, since the effective acoustic velocity in the fluid treatments is[22]

$$C_s \equiv \left(\frac{ZT_e + \gamma T_i}{m} \right)^{1/2}$$

and it is not obvious what to take for either γ or T_i. For the purposes of Figs. 18 and 19 we show our kinetic results when $T_{i\infty} = T_e$ and scale the fluid results by taking $C_s = \sqrt{2} V_s$. This means that the fluid results, which are limited to $|v| < C_s$, range over $-\sqrt{2} < u_d < \sqrt{2}$. One can think of this assumption as being that $\gamma = 1$ and the relevant ion temperature is the external value. However, the physics is probably much closer to the case of γ of order 2–2.5 and the effective ion temperature being 0.4–0.5 times $T_{i\infty}$.

On this basis, our results agree well with those from the fluid calculation of Hutchinson[21] (and disagree with those of Stangeby[20]). This is perhaps not surprising since Hutchinson's assumptions are essentially the fluid equivalents of the present kinetic model. The kinetic calculation gives slightly larger current, although not very significantly, in view of the uncertainties in the comparison. The present results extend to the supersonic case, while the fluid treatments do not.

In Fig. 19 we compare the ratio of upstream to downstream ion sheath current versus flow velocity with several other theories. We include the fluid theories of Hutchinson and of Stangeby and also the naive particle model of Harbour and Proudfoot[3] (essentially equivalent to that of Mott-Smith and Langmuir,[29] which takes the ion distributions at the probe to be drifted Maxwellians and ignores the presheath field effects). Also shown is the *ad hoc* empirical model of Proudfoot *et al.*,[5] which in our present normalization is $R = \exp(1.2 u_d)$. The ion temperature is taken equal to the electron temperature.

All these results give remarkably straight lines on a log-linear plot, as Fig. 19 shows. They may therefore be summarized in the form of a single slope K, in $R = \exp(K u_d)$, as Mott-Smith and Langmuir, $K \sim 2.7$; Proudfoot *et al.*, $K \sim 1.2$; Stangeby, $K \sim 0.8$; Hutchinson, $K \sim 1.75$; and our present calculation, $K \sim 1.7$.

V. CONCLUSION

We have developed a one-dimensional kinetic model for the flow of plasma ions to a probing object in a strong magnetic field. We use a new type of source term that treats consistently the diffusive cross-field fluxes. Ion parameters such as current, ratio of upstream to downstream current, density, fluid velocity, power flux, and potential variation along the presheath have been obtained. Our results agree well with Hutchinson's[21–23] fluid model, which incorporates diffusivity and viscosity, but give considerable additional information. The ion temperature variation along the flux tube is substantial and may be expressed as approximately adiabatic with $\gamma = 2$–2.5.

Our results extend the drift velocity from subsonic to supersonic. The parameters show a smooth change from subsonic to transonic cases. There is no evidence of a shock in the wake even for the case of low ion temperature and large drift velocity ($T_{i\infty} = 0.2 T_e$, and up to $u_d = 5$). However, it must be recalled that we are treating a very simplified one-dimensional model. Multidimensional effects in the wake may reveal much more complex physical structures.

The ratio of upstream to downstream sheath current can be expressed as an exponential of drift velocity [i.e., $J_{\rm up}/J_{\rm down} = \exp(K u_d)$], where K is ~ 1.7 for $T_{i\infty} = T_e$. This result provides a calibration for the measurement of plasma flow using Mach probes.

ACKNOWLEDGMENTS

We would like thank B. Lipschultz for many helpful discussions. The work was supported under U.S. Department of Energy contract No. DE/AC02-78et51013.

[1]G. M. McCracken and P. E. Stott, Nucl. Fusion **19**, 889 (1978).
[2]F. Wagner *et al.*, Phys. Rev. Lett. **49**, 1408 (1982).
[3]P. J. Harbour and G. Proudfoot, J. Nucl. Mater. **121**, 222 (1984).
[4]P. C. Stangeby, in *Physics of Plasma-Wall Interations in Controlled Fusion,* edited by D. E. Post and R. Behrisch (Plenum, New York, 1986), p. 41.
[5]G. Proudfoot, P. J. Harbour, J. Allen, and A. Lewis, J. Nucl. Mater. **128/129**, 180 (1984).
[6]A. S. Wan, B. LaBombard, B. Lipschultz, and T. F. Yang, J. Nucl. Mater. **145/147**, 191 (1987).
[7]U. Samir, R. H. Comfort, C. R. Chappell, and N. H. Stone, J. Geophys. Res. **91**, 5725 (1986).
[8]W. J. Raitt, J. V. Eccles, D. C. Thompson, P. M. Banks, P. R. Williamson, and R. I. Bush, Geophys. Res. Lett. **14**, 359 (1987).
[9]M. A. Morgan, C. Chan, and R. C. Allen, Geophys. Res. Lett. **14**, 1170 (1987).
[10]I. Katz and D. E. Parks, J. Spacecr. Rockets **20**, 22 (1983).
[11]D. Bohm, in *The Characteristics of Electrical Discharges in Magnetic Fields,* edited by A. Guthrie and R. K. Wakerling (McGraw Hill, New York, 1949), p. 77.
[12]I. H. Hutchinson, *Principles of Plasma Diagnostics* (Cambridge University Press, New York, 1987), Chap. 3.
[13]J. R. Sanmartin, Phys. Fluids **13**, 103 (1970).
[14]J. G. Laframboise and J. Rubinstein, Phys. Fluids, **19**, 1900 (1976).
[15]L. Tonks and I. Langmuir, Phys. Rev. **34**, 876 (1929).
[16]E. R. Harrison and W. B. Thompson, Proc. Phys. Soc. London **74**, 145 (1959).
[17]G. A. Emmert, R. M. Wieland, A. T. Mense, and J. N. Davidson, Phys. Fluids **23**, 803 (1980).
[18]R. C. Bissel and P. C. Johnson, Phys. Fluids **30**, 779 (1987).
[19]P. C. Stangeby, J. Phys. D **15**, 1007 (1982).
[20]P. C. Stangeby, Phys. Fluids **27**, 2699 (1984).
[21]I. H. Hutchinson Phys. Fluids **30**, 3777 (1987).
[22]I. H. Hutchinson, in Proceedings of the Fourteenth European Conference on Controlled Fusion and Plasma Physics, Madrid, 1987, Vol. 11D of European Conference Abstracts, edited by F. Engelmann and J. L. Alvarez Rivas (unpublished), Pt. III, p. 1330.
[23]I. H. Hutchinson Phys. Rev. A **37**, 4358 (1988).
[24]G. E. Forsythe and W. R. Wasow, *Finite Difference Methods for Partial Differential Equations* (Wiley, New York, 1960).
[25]M. J. M. Parrot, L. R. O. Storey, L. W. Parker, and J. G. Laframboise, Phys. Fluids **25**, 2388 (1982).
[26]Ya. B. Zel'dovich and Yu. P. Raizer, *Physics of Shock Wave and High Temperature Hydrodynamic Phenomena* (Academic, New York, 1966), Vol. I, Chap. 1.
[27]B. Bezzerides, D. W. Forslund, and E. L. Lindmann, Phys. Fluids **21**, 2178 (1978).
[28]D. Diebold, N. Hershkowitz, and S. Eliezer, Phys. Fluids **30**, 3308 (1987).
[29]H. M. Mott-Smith and I. Langmuir, Phys. Rev. **28**, 727 (1926).